www.czasopisma.pan.pl PAN POLSKA AKADEMIA NAUK www.journals.pan.pl

A R C H I V E S O F M E T A L L U R G Y A N D M A T E R I A L S

Volume 59 2014 Issue 2

DOI: 10.2478/amm-2014-0091

A. MILENIN*, M. GZYL*, T. REC*, B. PLONKA**

COMPUTER AIDED DESIGN OF WIRES EXTRUSION FROM BIOCOMPATIBLE Mg-Ca MAGNESIUM ALLOY

OPRACOWANIE ZA POMOCĄ MODELOWANIA NUMERYCZNEGO PROCESU WYCISKANIA CIENKICH PRĘTÓW Z BIOKOMPATYBILNEGO STOPU MAGNEZU, ZAWIERAJĄCEGO DODATEK Ca

Mathematical model of small-diameter wires extrusion from biocompatible MgCa08 (Mg – 0.8% Ca) magnesium alloy was developed in the current paper in order to determine window of allowable technological parameters. Compression and tensile tests were carried out within temperature range 250-400°C and with different strain rates to determine the fracture conditions for the studied alloy. Finite element (FE) analysis was used to predict the billet temperature evolution and material damage during processing. The extrusion model takes into account two independent fracture mechanisms: a) surface cracking due to exceeding of the incipient melting temperature and b) utilization of material formability. FE simulations with different initial billet temperatures and pressing speeds were performed in order to determine the extrusion limit diagram (ELD) for MgCa08 magnesium alloy. The developed ELD was used to select the parameters for the direct extrusion of wires with diameter of 1 mm. Then, the extrusion of twelve wires was conducted at 400°C with pressing speed 0.25 mm/s. It was reported that the obtained wires were free from defects, which confirmed the good agreement between numerical and experimental results.

Keywords: magnesium alloys, extrusion, ductile fracture, FE analysis

W pracy zaproponowano model matematyczny procesu wyciskania prętów o małych średnicach z biokompatybilnego stopu magnezu MgCa08 (Mg – 0.8% Ca). Na podstawie opracowanego modelu możliwy jest dobór parametrów technologicznych rozpatrywanego procesu. Model procesu wyciskania zawiera model do prognozowania utraty spójności materiału, który został opracowany w oparciu o próby spęczania oraz jednoosiowego rozciągania w zakresie temperatur 250-400°C dla różnych prędkości odkształcenia. W oparciu o metodę elementów skończonych (MES) przeprowadzona została analiza numeryczna rozkładu temperatury oraz wskaźnika wykorzystania odkształcalności materiału w procesie wyciskania. Zaproponowany model zawiera dwa możliwe mechanizmy utraty spójności: a) wynikający z lokalnego przekroczenia temperatury topnienia, b) wynikający z wyczerpania zapasu plastyczności. W oparciu o przeprowadzoną analizę MES procesu wyciskania dla różnych temperatur oraz prędkości wyciskania opracowano diagram ELM (extrusion limit diagram) dla stopu MgCa08. Na podstawie opracowanego diagramu ELM dobrano parametry procesu wyciskania prętów o średnicy 1 mm. Weryfikację modelu procesu wyciskania dla stopu MgCa08 wykonano w warunkach laboratoryjnych, gdzie przeprowadzono dwunasto żyłowy proces wyciskania prętów w temperaturze 400°C i prędkości 0.25 mm/s. Otrzymane pręty były wolne od wad, co potwierdziło dobrą zgodność pomiędzy wynikami numerycznymi i eksperymentalnymi.

1. Introduction

Biocompatible magnesium alloys are very promising materials for medical applications due to natural presence of magnesium in human body, mechanical properties similar to human bone and *in vivo* degradation via corrosion process [1]. Due to its high corrosion rate in human body fluids, pure magnesium cannot be used as a material for biodegradable implants. However, degradation time can be modified by addition of calcium to magnesium alloys without decreasing its biocompatibility [2, 3]. Biomechanical properties, biocompatibility, *in vivo* and *in vitro* corrosion of Mg-Ca alloys were studied in [4, 5].

Apart from the biocompatibility related issues, manufacturing implants from Mg-Ca alloys is still challenging due to their low formability, which can be attributed to hexagonal closed-packed (HCP) crystallographic structure. It was reported for magnesium alloys that the main deformation mechanisms at room temperature are slip on basal plane and twinning. Temperature increase is required to activate additional slip systems on prismatic and pyramidal planes [6, 7], which give rise to ductility enhancement. For instance, wire drawing of the examined MgCa08 alloy was successfully realised at temperatures above 250°C [8, 9]. Determination of optimal extrusion parameters is a difficult task. Influence of billet temperature, pressing speed and extrusion ratio on the quality of manufactured product is usually investigated [10, 11, 12, 13, 14]. Most of the available papers on magnesium extrusion present results obtained for AZ31 wrought magnesium alloy, which exhibits reasonably good formability [15]. The extru-

* AGH UNIVERSITY OF SCIENCE AND TECHNOLOGY, AL. A. MICKIEWICZA 30, 30-059, KRAKÓW, POLAND

** INSTITUTE OF NON-FERROUS METALS GLIWICE, LIGHT METALS DIVISION SKAWINA, 19 PILSUDSKIEGO STR., 32-050 SKAWINA, POLAND

sion of rods from MgCa08 was already carried out at elevated temperatures [16]. It was shown that material is very sensitive to variations in temperature and strain rate, e.g. increase in the extrusion speed from 2 mm/s to 8 mm/s led to massive material damage.

In [10], direct extrusion experiments were conducted in order to investigate temperature and ram speed influence on a surface cracking of extruded profiles and rods. It was shown that increase in pressing speed causes heat rise due to friction. Conclusion was drawn that cracking occurs on profile surface when the temperature reaches the incipient melting point. In [11], billet temperature evolution as a function of ram speed was studied. It was observed that increase in extrude temperature varied linearly with logarithmic ram speed, similar effect was reported in [13]. Presented results show that pressing speed and billet temperature have strong influence on extrude quality.

Finite element (FE) analysis is a commonly used tool to simulate metal forming processes. It was used to predict temperature evolution in extruding profile [11], extrusion force [13], metal flow and weld seam formation in the porthole die [12]. Simulations are usually preceded by mechanical tests of compression, tension or torsion in order to determine flow stress curves of examined material [17].

FE simulation can also be used to predict fracture occurrence during processing of magnesium alloys, this approach was successfully applied for sheet metal forming [18] and wire drawing [8, 19]. In [8], the material formability utilization criterion was used to determine optimal drawing parameters, similar approach was also presented in [20]. Multi scale method was proposed for modelling fracture during cold wire drawing [19]. Boundary element method was used to simulate microstructure evolution and the solution was coupled with FE simulation. According to the presented papers, development of a complex ductility model is necessary to model fracture behaviour of Mg alloys.

The aim of this work was to determine the window of allowable extrusion parameters for MgCa08 magnesium alloy. The mathematical model of small-diameter wires extrusion was developed in order to determine the extrusion limit diagram and select the extrusion parameters which allowed obtaining wires free from defects. Two fracture criteria were taken into account: exceeding of the incipient melting temperature on a surface of extruded rod and utilization of material formability. Direct extrusion of wires with diameter of 1 mm was conducted in order to experimentally verify obtained numerical results.

2. 2. Mathematical model of extrusion

Flow stress model for MgCa08 magnesium alloy was introduced using Hansel-Spittel equation:

$$\sigma_s = A \exp(-m_1 t)\, \varepsilon^{m_2} \dot{\varepsilon}^{m_3} \exp\left(\frac{m_4}{\varepsilon}\right)(1+\varepsilon)^{m_5 t} \exp(m_7 \varepsilon)\, \dot{\varepsilon}^{m_8 t} t^{m_9}, \tag{1}$$

where: ε – effective strain, $\dot{\varepsilon}$ – effective strain rate, t – temperature, $A$and $m_1 - m_9$ – empirical coefficients.

The proposed ductility model states that only limited amount of strain, called *critical deformation*, can be introduced to the material without damaging it. The fracture is not observed as long as the effective strain is smaller than the critical deformation:

$$\psi = \frac{\varepsilon}{\varepsilon_p(k_\sigma, t, \dot{\varepsilon})} < 1, \tag{2}$$

where: ψ – ductility function, ε_p – critical deformation function.

Critical deformation was proposed as a function of stress triaxiality $k_\sigma = \sigma_0/\sigma_s$, temperature t and effective strain rate $\dot{\varepsilon}$:

$$\varepsilon_p(k_\sigma, t, \dot{\varepsilon}) = d_1 \exp(-d_2 k_\sigma) \exp(d_3 t)\, \dot{\varepsilon}^{d_4}, \tag{3}$$

where: d_1-d_4 – empirical coefficients.

It was assumed that two conditions must be satisfied to avoid material damage during processing. Maximum value of ductility function (2) is less than one and maximum calculated temperature is less than the incipient melting temperature of MgCa08 magnesium alloy, which is 516°C.

The solution of FE problem is based on the Norton-Hoff constitutive law [21, 22] and is described in [23]. This law is generally written in the form of relationship between stress tensor (σ) and the strain rate tensor ($\dot{\boldsymbol{\varepsilon}}$):

$$\boldsymbol{\sigma} = 2K\left(\sqrt{3}\dot{\varepsilon}\right)^{m-1} \dot{\boldsymbol{\varepsilon}} \tag{4}$$

The value of $m = 1$ corresponds to the Newtonian fluid with a viscosity $\eta = K$, when $m = 0$ equation (4) is equivalent to the plastic flow rule for a rigid-plastic material obeying the Levy-Mises flow rule and the Huber-Mises yield criterion. In the present paper the m value is strain rate sensitivity and is equal to m_3 coefficient, determined using inverse analysis. Relation between the yield stress and the constant K is:

$$K(t, \varepsilon, \dot{\varepsilon}) = \frac{\sigma_s}{\sqrt{3}^{m+1}\dot{\varepsilon}^m} \tag{5}$$

3. Experimental procedure

Tensile and compression samples were machined from hot-extruded rod with diameter of 30 mm, the material used was MgCa08 (Mg – 0.8% Ca) magnesium alloy. The dimensions of tensile samples were 5 mm of diameter and 25 mm strain gauge length. The diameter of compression specimens was 8 mm and 10 mm height. Both experiments were carried out on Zwick Z250 testing machine. Mechanical tests were conducted with different tool velocities: 1 mm/s and 10 mm/s within temperature range 250-400°C, as shown in TABLE 1.

TABLE 1

Tension and compression tests conditions

Sample no.	Sample temperature, °C	Tool velocity, mm/s
1	400	10
2	300	1
3		10
4	250	1
5		10

Load-displacement curves obtained from compression tests were used to identify empirical coefficients of the flow

stress model described by equation (1). Coefficients of the critical deformation function (3) were determined from the results of tension and compression. The maximum value of the critical deformation was expected to occur in the fracture initiation area. This area was localised on the basis of mechanical test results. The FE models of tension and compression were developed in order to identify values of strain, strain rate, temperature and stress triaxiality in the fracture initiation zone. Simulations were run in Forge3 commercial FE software. Then, optimization procedure was used to identify the empirical parameters of the flow stress and ductility models.

The identified models were implemented to Forge3 and FE simulations of wires extrusion were run in order to determine the extrusion limit diagram (ELD) for MgCa08 magnesium alloy. The diagram enabled selection of the extrusion parameters, initial billet temperature and pressing speed, which ensured fracture avoidance. The process was realised on the hydraulic press with load capacity 500 kN. Therefore, another constraint was that the maximum extrusion force should have not exceeded this value. Direct extrusion of wires 1 mm diameter was conducted in order to verify FE simulation results.

4. Mechanical tests results

Tensile and compression tests were run to failure in order to identify the fracture initiation point in the samples. The experimental and numerical results showed that first cracks are observed in the middle of the tensile sample and on the edge of the cylindrical compression sample. The results obtained from experiments enabled to identify conditions of the material damage for negative and positive stress triaxialities, respectively. The maximum values of calculated local fracture strain were 1.9 in compression and 2.5 in tension. The stress triaxiality varies from 0.6 to -1.2 for different tests. The maximum local strain rate at failure was calculated for compression at 400°C and was equal to 5 s^{-1}. The results obtained from the mechanical tests and corresponding FE simulations are shown in TABLE 2.

TABLE 2
Results obtained from mechanical test and corresponding FE simulations

t, °C	v, mm/s	Fracture strain, –		Stress triaxialit y at fracture, –		Strain rate at fracture, s^{-1}	
		C	T	C	T	C	T
400	10	1.9	2.5	-1.2	0.6	5	3.6
300	1	1.56	2.35	-0.6	0.6	0.5	0.8
	10	1.56	1.18	-0.6	0.58	3.3	3.8
250	1	1.7	0.66	-0.8	0.5	0.9	0.1
	10	0.87	0.41	-0.57	0.35	3	0.66

C – compression, T – tension, t – temperature, v – tool velocity

5. Optimization procedure

5.1. Flow stress model

The compression tests results were used to identify parameters of the flow stress model. The Hooke-Jeeves algorithm was used to minimize the objective function, defined as root mean square error between the load curves obtained from experiment and predicted by FE simulation. Friction factor in simulation was equal to 0.1. Coefficients of equation (1), determined using the optimization method, are as follows: A =405.85; m_1 =-0.00826428; m_2 =-0.0281807; m_3 =0.020492; m_4 =-0.0114059; m_5 =0.00521939; m_7 =-0.69316; m_8 =0.0001636; m_9 =0.192958. Figure 1 shows the comparison between the load curves obtained from compression tests and their prediction calculated in Forge3.

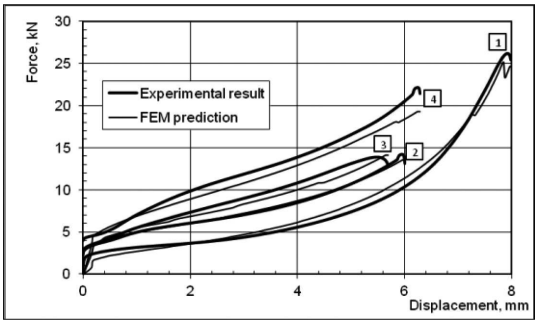

Fig. 1. Force-displacement curves obtained from compression tests 1-4 and their prediction calculated using flow stress given by equation (1)

5.2. Ductility model

The generalized reduced gradient algorithm for nonlinear problems implemented in MS Excel Solver was used to determine the empirical coefficients of the critical deformation function. According to equation (3), the ductility function in a fracture initiation zone should be equal to or greater than one to correctly predict the material damage. Therefore, the objective function was defined using the following equation:

$$\Phi = \frac{1}{n}\sum_{i=1}^{n}(1-\psi_i)^2, \tag{6}$$

where: ψ_i – value of ductility function in fracture initiation zone obtained from FE simulation, n – number of measurements.

The empirical coefficients of equation (3) are as follows: d_1 =0.04611; d_2 =0.4759; d_3 =0.01265; d_4 =-0.07009. Comparison between the real fracture strain obtained from experiments and the ductility model prediction is shown in Figure 2. Test numbers correspond to the results presented in Table 1. Total percentage error between real and calculated values was 7.8%. The overestimation of predicted critical strain was observed for sample compressed at 400°C. It was caused by significant ductility increase along with temperature rise, which was difficult to capture in optimisation procedure. Nevertheless, this sample did not undergo massive shear damage as it was observed for specimens tested at lower temperatures. Therefore, it can be concluded that the model can still give reasonable prediction of material ductility at 400°C.

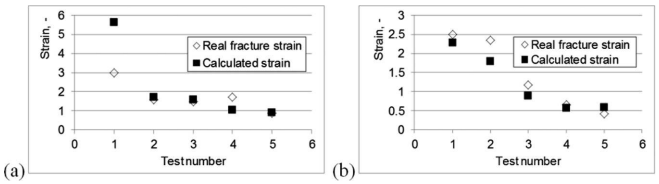

Fig. 2. Comparison between the critical strain values obtained from the experiments and FE simulations: (a) compression tests; (b) tensile tests

Figure 3 shows the comparison between results obtained from FE simulation and tensile test carried out at 300°C with tool velocity 1 mm/s. The model predicted that ductility function value was greater than one when total tool displacement reached 22 mm (Fig. 3a). During experimental testing the sample fractured at displacement 22.5 mm (Fig. 3b).

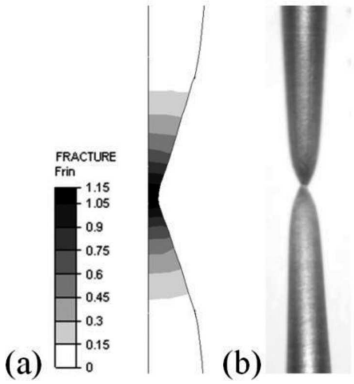

Fig. 3. Tensile test at 300°C with tool velocity equal to 1 mm/s: (a) ductility function; (b) fractured specimen.

The relationship between critical deformation function and temperature is shown in Fig. 4a. Critical deformation raises along with temperature increase, therefore, probability of fracture occurrence decreases. Large strain, which is usually observed in extrusion process, can be introduced to material without damaging it at temperature as high as 350-400°C. Therefore, there is no point in running simulations of extrusion process for temperatures lower than 350°C. Figure 3b shows the influence of stress triaxiality on critical deformation. It is apparent that in the zones where tensile stress dominates, which is equivalent to positive value of stress triaxiality, material is more prone to damage comparing to negative stress triaxiality zones.

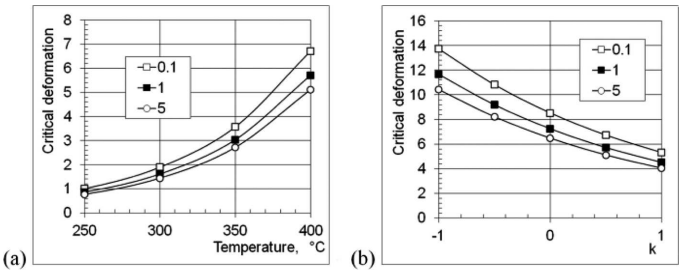

Fig. 4. Critical deformation for different temperatures (a), stress triaxialities (b) and strain rates

6. FE simulation of extrusion

6.1. Model details and experimental plan

The identified flow stress and ductility models were used in Forge3 to perform FE simulations of wires extrusion. The ductility model was implemented into Forge3 using FORTRAN user subroutines. Current values of temperature, effective strain, effective strain rate and flow stress can be obtained directly as predefined FORTRAN variables. Flat die with twelve orifices 1 mm diameter was proposed for the process, as shown in Figure 5. The billet from MgCa08 was 40 mm long with diameter of 30 mm. Friction between billet and dies was described using Tresca friction law with friction factor equal to 0.5. Due to the model symmetry only 1/12 part of the model was calculated, which allowed reducing computation time significantly.

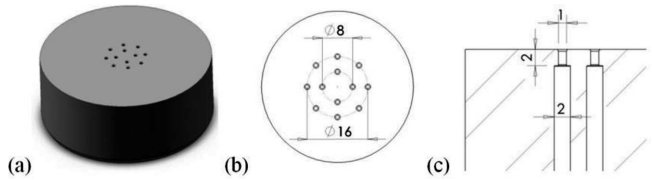

Fig. 5. The die used in the FE simulation of extrusion process: a) 3D model; b) top view; c) broken-out section (all dimensions are in mm)

The goal of the performed FE analysis was to identify the window of allowable extrusion parameters of small-diameter wires extrusion. The influence of initial billet temperature and pressing speed on material ductility and force needed to conduct the process was studied. Simulations were run with initial billet temperatures: 350, 400, 450°C and pressing speeds: 0.25, 0.5 and 1 mm/s, which gives nine simulation variants in total.

6.2. Extrusion limit diagram

The FE simulation results were used to determine the extrusion limit diagram (ELD) for MgCa08 magnesium alloy. The maximum value of ductility function and the maximum temperature on billet surface were obtained from every simulation. Those values were plotted on the diagram shown in Fig. 6. Solid and hollow marks show the values of ductility function and maximum billet temperature, respectively. Moreover, solid line which indicates the formability limit (ductility function equal to one) and dashed line showing the incipient melting point equal to 516°C were plotted.

It is apparent from Figure 6 that the maximum local value of ductility function was less than one for four from nine investigated variants. Extrusion can be carried out at 450°C with pressing speed 1 mm/s but processing at 400°C requires lowering velocity to 0.25 mm/s. It was predicted that conducting the process at 350°C leads to material damage. The maximum temperature did not exceed the melting point in any of the performed simulations; it reached 476°C during pressing with 1 mm/s at 450°C. The risk of local material melting is smaller than fracture occurrence due to limited ductility of MgCa08 at investigated temperatures. Generally, extrusion of small-diameter wires is possible to realise at 400°C with low

pressing speed and temperature increase is required to speed up the process and improve efficiency.

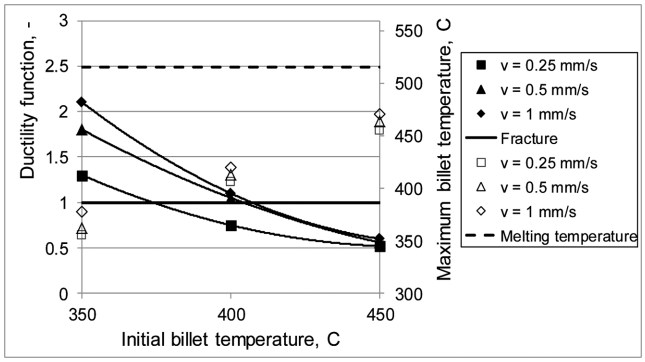

Fig. 6. Extrusion limit diagram for MgCa08 magnesium alloy. The solid marks represent the ductility function and the hollow marks show the maximum temperature values

The ELD allows determining the extrusion parameters which ensure that produced wires will not be damaged. However, another parameter that should be considered is a maximum force needed to conduct the process as each press has its load capacity. The maximum extrusion force obtained from FE simulations was plotted in Figure 7. Extrusion at 350°C requires a press with load capacity of 600 kN, further temperature increase reduces this value to ~500 kN and ~430 kN for 400°C and 450°C, respectively. Moreover, lowering pressing speed also reduces the maximum extrusion force in each case and it is explained by the material strain rate sensitivity at elevated temperatures. Solid line in Fig. 7 indicates the load capacity of the press used for experimental verification of presented FE simulation results.

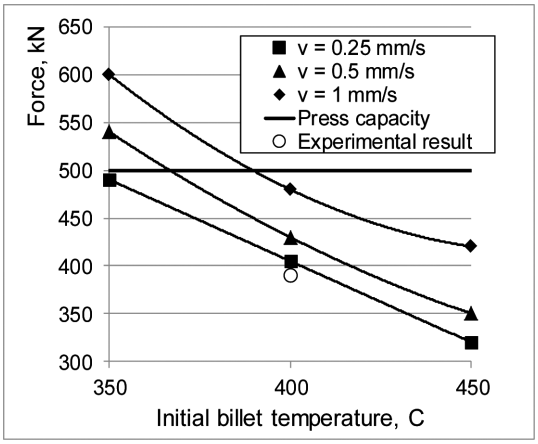

Fig. 7. Numerical prediction of the maximum extrusion force and the maximum force measured during extrusion conducted at 400°C with pressing speed 0.25 mm/s

Figure 8 shows the results obtained from FE simulation with initial billet temperature 400°C and pressing speed 0.25 mm/s. Due to the low ram velocity, temperature rose only up to 406°C. The maximum values are observed in the billet volume; therefore, heat generation due to the friction in the die orifice was negligible. It is important since the heat generation on billet-die interface is often a main cause of local temperature rise and crack occurrence during extrusion process [9]. Figure 8c shows mean stress field obtained from simulation; die orifice is a tensile stress dominated zone which coincides with the region where the maximum critical deformation occurs. It indicates that tensile stress field observed in the die orifice during extrusion is responsible for material damage.

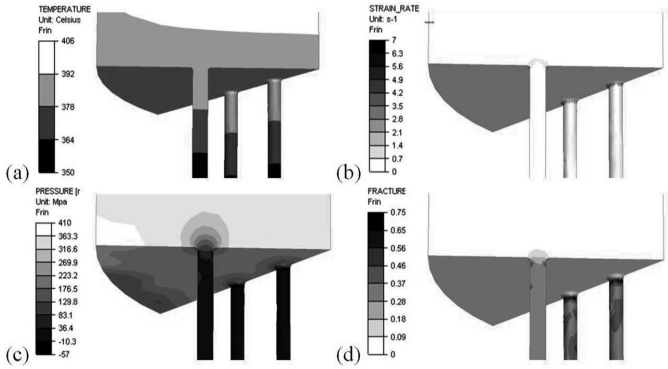

Fig. 8. Results of the FE simulation with initial billet temperature 400°C and pressing velocity 0.25 mm/s: (a) temperature; (b) effective strain rate; (c) mean stress; (d) ductility function

7. Extrusion of wires

The extrusion of wires with diameter of 1 mm from MgCa08 magnesium alloy was conducted at 400°C with pressing speed 0.25 mm/s. According to the developed ELD, the selected parameters guarantee that obtained wires will not fracture during processing. The experiment was realised using the hydraulic press with load capacity of 500 kN, which is shown in Fig. 9. The FE analysis showed that extrusion force does not exceed the press capacity for the selected parameters. Die used in the process is shown in Fig. 5, the billet dimensions were 30 mm diameter and 40 mm length. The graphite grease was used as a lubricant.

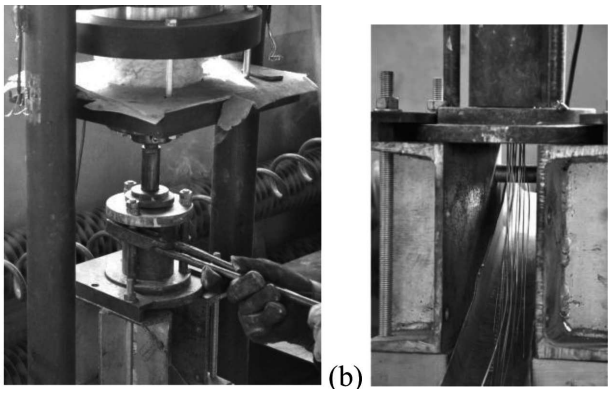

Fig. 9. The hydraulic press (a) and the extrusion of twelve wires from MgCa08 (b)

Twelve wires were obtained by direct extrusion and cracks were not observed on the wires surface after processing; one of the produced wires is shown in Fig. 10. The maximum load during extrusion was measured as 390 kN which gives the good agreements with FE prediction (405 kN), as shown in Fig. 7. Tensile test was performed on Instron 4502 testing machine in order to investigate the wire strength and ductility. Mechanical properties of the examined wires are: yield stress –

151 MPa, ultimate tensile stress – 227 MPa, Young's modulus – 19.85 GPa and elongation to failure 19.4% (obtained using 50 mm gauge length).

Fig. 10. The wire produced by extrusion process

8. Conclusions

The aim of the present work was to determine the extrusion limit diagram (ELD) for MgCa08 biocompatible magnesium alloy. FE simulations of 1 mm diameter wires extrusion with different billet temperatures and pressing speeds were run in order to identify when the extruded material starts to fracture. Mechanical tests of tension and compression were carried out in order to obtain reliable input data for simulations. The developed ductility model takes into account two independent fracture mechanisms: surface cracking due to exceeding of the incipient melting temperature and the utilization of material formability.

It was apparent from the developed ELD that extrusion can be realised without fracture occurrence at 400°C with the low pressing speed. Processing with higher velocities requires temperature increase up to 450°C. It was also predicted that the extrusion force does not exceed 500 kN as long as the both conditions are fulfilled: the billet temperature is at least 400°C and the pressing speed is less than 1 mm/s. The direct extrusion of twelve wires with diameter of 1 mm was successfully conducted at 400°C with velocity 0.25 mm/s. The obtained wires were free from defects, which confirmed the good agreement between experimental results and numerical prediction.

Acknowledgements

Financial assistance from the National Science Centre of Poland, project no. 2012/05/B/ST8/01797 is acknowledged.

REFERENCES

[1] M.P. Steiger, A.M. Pietak, A.M. Huadmai, G. Dias, Biomaterials **27**, 1728 (2006).
[2] K. Feser, M. Kietzmann, M. Baeuemer, C. Krause, F.-W. Bach, J. Biomater. Appl. **25**, 685 (2011).
[3] N. von der Hoh, A. Krause, C. Hackenbroich, D. Bormann, A. Lucas, A. Meyer-Lindenberg, Dtsch. Tierarztl. Wochenschr. **113**, 439 (2006).
[4] A. Drynda, J. Seibt, T. Hassel, F.-W. Bach, M. Peuster, J. Biomed. Mater. Res. A **101A**, 33 (2012).
[5] N. Erdmann, N. Angrisani, J. Reifenrath, A. Lucas, F. Thorey, D. Bormann, A. Meyer-Lindenberg, Acta Biomater. **7** , 1421 (2011).
[6] F. Yoshinaga, R. Horiuchi, Trans. JIM **4**, 1 (1963).
[7] B.C. Wonsiewicz, W.A. Backofen, Trans. TMS-AIME **239**, 1422 (1967).
[8] A. Milenin, P. Kustra, Archives of Metallurgy and Materials, **58**(1), 55 (2013).
[9] J.-M. Seitz, D. Utermohlen, E. Wulf, C. Klose, F.-W. Bach, Adv. Eng. Mater. **13**, 1087 (2011).
[10] R.Ye. Lapovok, M.R. Barnett, C.H.J. Davies, J. Mater. Process. Tech. **146**, 408 (2004).
[11] G. Liu, J. Zhou, J. Duszczyk, J. Mater. Process. Tech. **186**, 191 (2007).
[12] G. Liu, J. Zhou, J. Duszczyk, J. Mater. Process. Tech. **200**, 185 (2008).
[13] G. Liu, J. Zhou, J. Duszczyk, T. Nonferr, Metal Soc. **18**, 247 (2008).
[14] W. Tang, S. Huang, S. Zhang, D. Li, Y. Peng, J. Mater. Process. Tech. **211**, 1203 (2011).
[15] H.Y. Chao, Y. Yang, X. Wang, E.D. Wang, Mat. Sci. Eng. Struct A **528**, 3428 (2011).
[16] A. Milenin, J.-M. Seitz, F.-W. Bach, D. Bormann, P. Kustra, Wire Journal Int. **6**, 74 (2011).
[17] L. Li, J. Zhou, J. Duszczyk, J. Mater. Process. Tech. **172**, 372 (2006).
[18] W.J. Kim, H.K. Kim, W.Y. Kim, S.W Han, Mat. Sci. Eng. A-Struct **488**, 468 (2008).
[19] A. Milenin, D. Byrska, O. Gridin, Computers & Structures **89**, 1038 (2011).
[20] F. Grosman, M. Tkocz, Arch. Civ. Mech. Eng. **4**, 77 (2004).
[21] N.J. Hoff, Journal of Applied Mathematics **12**, 49 (1954).
[22] F.H. Norton, Creep of Steel at High Temperature, McGraw Hill, New York 1929.
[23] J.-L. Chenot, M. Bellet, in: P. Hartley, I. Pillinger, C.E.N. Sturgess (Eds.), Numerical Modelling of Material Deformation Processes: Research, Developments and Applications, Springer-Verlag, London, 1992.

Received: 20 March 2014.